CX3CL1/CX3CR1 axis alleviates inflammation and apoptosis in human nucleus pulpous cells via M2 macrophage polarization

XIAO-WEN GAO[1*], HAN-LIN HU[1*], MING-HUA XIE[1*], CAI-XIA TANG[2], JUN OU[1] and ZHENG-HAO LU[1]

[1]The Department of Spinal Surgery and [2]The Department of Obstetrics and Gynecology, Affiliated Nanhua Hospital, University of South China, Hengyang, Hunan 421001, P.R. China

Received September 14, 2022; Accepted April 6, 2023

DOI: 10.3892/etm.2023.12058

Abstract. CX3C chemokine ligand 1 (CX3CL1) belongs to the CX3C chemokine family and is involved in various disease processes. However, its role in intervertebral disc degeneration (IDD) remains to be elucidated. In the present study, western blotting, reverse transcription-quantitative PCR and ELISA assays were used to assess target gene expression. In addition, immunofluorescence and TUNEL staining were used to assess macrophage infiltration, monocyte migration and apoptosis. The present study aimed to reveal if and how CX3CL1 regulates IDD progression by exploring its effect on macrophage polarization and apoptosis of human nucleus pulposus cells (HNPCs). The data showed that CX3CL1 bound to CX3C motif chemokine receptor 1 (CX3CR1) promoted the M2 phenotype polarization via JAK2/STAT3 signaling, followed by increasing the secretion of anti-inflammatory cytokines from HNPCs. In addition, HNPC-derived CX3CL1 promoted M2 macrophage-derived C-C motif chemokine ligand 17 release thereby reducing the apoptosis of HNPCs. In clinic, the reduction of mRNA and protein levels CX3CL1 in degenerative nucleus pulposus tissues (NPs) was measured. Increased M1 macrophages and pro-inflammatory cytokines were found in NPs of IDD patients with low CX3CL1 expression. Collectively, these findings suggested that the CX3CL1/CX3CR1 axis alleviates IDD by reducing inflammation and apoptosis of HNPCs via macrophages. Therefore, targeting CX3CL1/CX3CR1 axis is expected to produce a new therapeutic approach for IDD.

Correspondence to: Professor Zheng-Hao Lu or Professor Jun Ou, The Department of Spinal Surgery, Affiliated Nanhua Hospital, University of South China, Dongfeng Road, Hengyang, Hunan 421001, P.R. China
E-mail: luzhenghao@163.com
E-mail: 785950353@qq.com

*Contributed equally

Key words: CX3C chemokine ligand 1, CX3C motif chemokine receptor 1, intervertebral disc degeneration, macrophage, inflammation, apoptosis

Introduction

Intervertebral disc degeneration (IDD) is a universal chronic disease that is frequently characterized by back pain (1). Complicated pathogenic mechanisms increase the therapeutic difficulties of IDD (2,3). The inflammatory response and apoptosis in nucleus pulposus cells (NPCs) promote the degradation of NP tissues (4-7). Therefore, identifying the regulators of inflammation and apoptosis in NPCs should improve the prevention and treatment of IDD.

Chemokine families are regularly of significant activity in research due to their important roles in various disease processes. CX3 chemokine ligand 1 (CX3CL1) belongs to the CX3 chemokine family and exerts its biological effects by binding to the specific receptor CX3C motif chemokine receptor 1 (CX3CR1) (8-10). The anti-inflammatory and anti-apoptotic roles of CX3CL1 have been discovered in different diseases (11,12). Although the mRNA expression of CX3CL1 and the CX3CR1 axis has been detected in the nucleus pulpous tissues (NPs) of cervical and lumbar vertebrae, the effect of the CX3CL1/CX3CR1 axis on IDD progression remains to be elucidated (13).

Macrophages play crucial roles in multiple pathophysiological processes, including IDD (14-20). Several studies have reported that p38 in NPCs regulates macrophage polarization and polarized macrophages are involved in IDD progression (14,20,21). Regulation of the phenotypic transition of infiltrated macrophages (M1 proinflammatory and M2 anti-inflammatory phenotypes) is important for controlling tissue inflammation (22,23). Nakazawa *et al* (24) detected M2 macrophage accumulation in degenerative intervertebral discs and positive staining significantly correlated with degenerative grades. In addition, Li *et al* (25) reported that M2 macrophage-conditioned medium alleviated IDD. Therefore, it is unclear how monocyte migration and macrophage polarization occur in NPs during IDD (26,27). Meanwhile, factors released from polarized macrophages have been shown to regulate apoptosis and further investigation of whether and how infiltrated macrophages affect apoptosis in HNPCs will be valuable (28,29). The CX3CL1/CX3CR1 axis affects macrophage chemotaxis and it would be useful to explore the association of the CX3CL1/CX3CR1 axis with macrophages and IDD.

The present study evaluated the role of macrophages in IDD and further assessed the involvement of macrophages in the molecular mechanism of the IDD process. In addition, the present study assessed the contribution of the CX3CL1/CX3CR1 axis to the development of IDD and the underlying communication of human nucleus pulposus cells (HNPCs) with macrophages during IDD. The studies were intended to provide a new way for IDD therapy in the future.

Materials and methods

Patient samples. The degenerative nucleus pulposus (NP) tissues were obtained from IDD patients [n=5 (female, 2; and male, 3); age range 29-74 years, median age 58 years] undergoing posterior lumbar interbody fusion (PLIF) due to degenerative lumbar disc disease in The Affiliated Nanhua Hospital of University of South China. The control NP tissues were obtained from lumbar vertebrae fracture patients without IDD [n=5 (female, 2; and male, 3); age range 14-65 years; median age 54 years] in The Affiliated Nanhua Hospital of University of South China. Voluteers were recruited between February and December 2021. The present study protocol conformed to the globally accepted regulations on clinical studies involving human data, and approval was conferred by the ethics committee of University of South China (approval no. 2021-ky-41). Written informed consent was obtained from all of the participants or donors' families before using the samples.

Immunofluorescence staining. Human NP tissue sections were incubated with UV block (Pierce; Thermo Fisher Scientific, Inc.) containing 10% goat serum (Abcam) for 30 min at room temperature and then with mouse cluster of differentiation (CD)68 (1:200, cat. no. ab283654, Abcam) overnight in a humid chamber at 4˚C. After, sections were incubated with a secondary antibody (1:500, cat. no. ab150077, Abcam) for 2 h at room temperature. Nuclei were counterstained with DAPI. After washing with PBS for 15 min, images were captured at x200 magnification on an Olympus FV1000 (Olympus Corporation).

Cell culture and transfection. HNPCs and THP-1-derived monocytes were purchased from Cell Bank of the Chinese Academy of Sciences (Shanghai, China) and cultured in DMEM or 1640 supplemented with 0.1% nonessential amino acids, penicillin (100 U/ml), streptomycin (100 mg/ml) and 10% FBS at 37˚C for 24 h. 100 ng/ml TNF-α (MedChemExpress) or 200 nmol/l PMA (MilliporeSigma) were used for inducing apoptosis of HNPCs and the differentiation of THP-1 derived monocytes into macrophages, respectively. Control vector and CX3CL1 and CCL17 overexpression vectors were packaged and purchased from Hanbio Biotechnology Co., Ltd. The 293T cell line from ATCC was used for generating viral particles. The mass of used vectors included 10 μg pHBLV, 10 μg psPAX2 and 5 μg pMD2G. HNPCs and THP-1-derived macrophages were cultured in 6-well plate at 37˚C with 5% CO_2. When cells reached 40-50% confluence, 1 ml of serum-free medium was replaced with serum-containing medium and $2x10^8$ TU/ml viral particles [HNPC (MOI: 30) and THP-1-derived macrophage (MOI: 10)]. After 12 h, 1 ml of serum-containing medium was added to wells and the medium changed to fresh serum-containing medium at 24 h. After 48 h, puromycin was used for screening of stably transfected cells. The stably expressed cells were screened using 4 μg/ml puromycin for 7 days followed by use for different experiments. The generation used of transfected cells were controlled at third generation. Cells were incubated with CX3CR1 inhibitor JMS-17-2 (MedChemExpress) or JAK2/STAT3 inhibitor SD1029 (MedChemExpress).

Reverse transcription-quantitative (RT-q) PCR. Human nucleus pulpous cells and THP-1-derived macrophages were cultured in 6-well plates at 37˚C and were used for RNA extraction when the confluent reached ~95%. The RNA extraction, complementary DNA (cDNA) synthesis, and qPCR were performed according to the manufacturer's protocols. Human nucleus pulpous cells, THP-1-derived macrophages and NPs were treated and lysed for RNA extraction using the TRIzol® (Thermo Fisher Scientific, Inc.) extraction method. Total RNA was reversed transcribed into cDNA with HiScript III RT SuperMix (R323-01, Vazyme). qPCR amplifications were performed according to manufacture manual from ChamQ SYBR qPCR Master Mix (cat. no. RQ311-02; Vazyme Biotech Co., Ltd.), which was 95˚C for 30 sec, 95˚C 5 sec, 60˚C 20 sec for additional 40 cycles. Using 18s as a control, the $2^{-\Delta\Delta Cq}$ method was applied to calculate the relative mRNA expression of target genes. The sequences of the primers were: Human CX3CL1, 5'-GCC ACAGGCGAAAGCAGTA-3' and 5'-GGAGGCACTCGG AAAAGCTC-3'; Human CX3CR1, 5'-AGTGTCACCGAC ATTTACCTCC-3' and 5'-AAGGCGGTAGTGAATTTG CAC-3'; Human CD86: 5'-AGTGGAATAGCCTCCCTG TAACTCC-3' and 5'-CCCATAAGTGTGCTCTGAAGT GAAA-3', Human CD206: 5'-TCCGGGTGCTGTTCTCCT A-3', 5'-TCCGGGTGCTGTTCTCCTA-3'; Human IL-1β: 5'-ATGATGGCTTATTACAGTGGCAA-3' and 5'-GTC GGAGATTCGTAGCTGGA-3', Human IL-6: 5'-ACTCAC CTCTTCAGAACGAATTG-3' and 5'-CCATCTTTGGAA GGTTCAGGTTG-3', Human IL-4: 5'-CGGCAACTTTGT CCACGGA-3' and 5'-TCTGTTACGGTCAACTCGGTG-3', Human IL-10: 5'-GACTTTAAGGGTTACCTGGGTTG-3' and 5'-TCACATGCGCCTTGATGTCTG-3' and 18s: 5'-TTG ACGGAAGGGCACCACCAG-3' and 5'-GCACCACCACCC ACGGAATCG-3'. Analysis of mRNA levels was performed using ABI PRISM7900 sequence detection system (Applied Biosystems; Thermo Fisher Scientific, Inc.).

Monocyte migration. THP-1-derived monocytes were added to the upper chamber and culture supernatant to the lower chamber of 5.0 μm Transwell inserts (Corning, Inc.). The number of migrated cells was assessed after 24 h by incubating with calcein at 37˚C and positive cells in low chambers counted. Fluorescence microscopy images were captured at x200 magnification on an Olympus BX-53-LV2000 (Olympus Corporation).

TUNEL assay. TUNEL staining was used to evaluate cell apoptosis. The cells were fixed in 4% paraformaldehyde for 1 h at room temperature and then treated with 0.5% TritonX-100

for 10 min. After washing with PBS, the cells were incubated with the cell death detection kit (Elabscience Biotechnology, Inc.) according to the manufacturer's instructions. Nuclei were counterstained with DAPI (Beyotime Institute of Biotechnology). Fluorescence microscopy images were captured at x200 magnification on an Olympus BX-53-LV2000 (Olympus Corporation).

Western blot analysis. Total protein were extracted with RIPA cell lysis buffer (Beyotime Institute of Biotechnology) and Protease and Phosphatase Inhibitor Cocktail (MedChemExpress) on ice for 30 min and centrifuged at 13,400 x g for 10 min at 4˚C. Total protein were quantified by a BCA kit (Beyotime Institute of Biotechnology). Primary antibodies included anti-CX3CL1 (Proteintech Group, Inc.; cat. no. 10108-2-AP; 1:1,000), anti-CX3CR1 (Proteintech Group, Inc.; cat. no. 13885-1-AP; 1:1,000), BCL-2 (Proteintech Group, Inc.; cat. no. 68103-1-Ig; 1:1,000), Bax (Proteintech Group, Inc.; cat. no. 50599-2-Ig; 1:1,000), anti-STAT3 (Abcam; cat. no. ab68153; 1:200), anti-phosphorylated (p-)STAT3 (Abcam; cat. no. ab76315; 1:1,000), anti-JAK2 (Abcam; cat. no. ab108596; 1:1,000), anti-p-JAK2 (Abcam; cat. no. ab32101; 1:1,000), anti-GAPDH (Abcam; cat. no. ab8245; 1:2,000) and anti-β-actin (Abcam; cat. no. ab8226; 1:2,000). Secondary antibodies were HRP-labelled Goat anti-Mouse or anti-Rabbit IgG (H + L) (Abcam; cat. no. ab6789 or ab6721; 1:5,000). The amount of GTP bound RHOA in cell-free lysates was determined using the RHO Activation Assay kit (MilliporeSigma). Protein (30 μg) of each sample were electrophoresed via 12% SDS gel and transferred to polyvinylidene fluoride membrane (MilliporeSigma). The membranes were blocked with 5% fat-free milk for 1 h at room temperature, incubated with indicated primary antibodies overnight at 4˚C and incubated with HRP-conjugated secondary antibodies at room temperature for 2 h. Antibody binding was visualized with Tanon 5500 (Tanon Science and Technology Co., Ltd.) and BeyoECL Plus (Beyotime Institute of Biotechnology), and ImageJ software (version 1.8.0.112; National Institutes of Health) was used for analyzing the blots.

ELISA assay. Supernatant from treated HNPCs and THP-1-derived macrophages were collected and centrifuged at 2,000 x g for 10 min. The supernatants then were used to ELISA according to the instruction of kits (cat. nos. CX3CL1, ab192145; IL-4, ab215089; IL-10, ab185986; CCL17, ab183366; Abcam).

Statistical analysis. All data were presented as means ± SD. Statistical significance was evaluated by either one-way ANOVA or Student's t-test. Student's t-test was used for assessing the differences between two groups, while one-way ANOVA with Scheffe's test was used for analyzing the difference among multiple groups. P<0.05 was considered to indicate a statistically significant difference.

Results

CX3CL1 is downregulated in human degenerative NPs. To identify whether CX3CL1 contributed to IDD, the levels of CX3CL1 were detected in NPs of IDD patients. As shown in Fig. 1A and B, the mRNA and protein levels of CX3CL1 were significantly decreased in degenerative NP tissues. However, CX3CR1 expression in degenerative NPs were unchanged (Fig. 1C and D). This indicated that CX3CL1 might possess a potential regulatory effect on IDD progression.

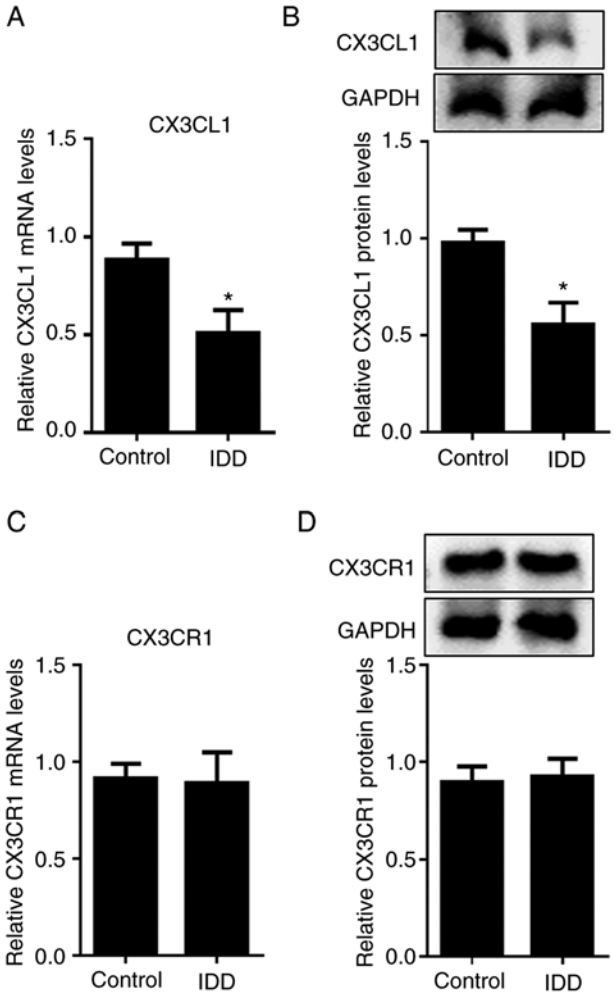

Figure 1. CX3CL1 expression is reduced in degenerative NP tissues. Analysis of (A) mRNA and (B) protein levels of CX3CL1 in NPs via RT-qPCR and western blotting. Analysis of (C) mRNA and (D) protein levels of CX3CR1 in NPs via RT-qPCR and western blotting. All data were shown as mean ± SD from five independent experiment with each performed in triplicate. *P<0.05 vs. Control group. CX3CL1, CX3C chemokine ligand 1; NPs, nucleus pulposus tissues; RT-qPCR, reverse transcription-quantitative PCR.

HNPC-derived CX3CL1 promotes monocyte migration via CX3CR1. Macrophages have been reported to be involved in inflammatory response during IDD progression (30,31). As shown in Fig. 2A, abundant CD68 positive fluorescence staining was detected in NPs of IDD patients. Given that the tissue macrophages are mainly derived from circulating monocytes, the present study aimed to identify whether CX3CL1 was involved the regulation of monocyte migration. As shown in Fig. 2B-E, HNPC supernatant significantly promoted THP-1-derived monocytes migration and overexpression of CX3CL1 markedly promoted this effect. Furthermore, CX3CR1 antagonist JMS-17-2 significantly blocked CX3CL1 overexpression and supernatant-induced THP-1-derived monocytes migration (Fig. 2D-E). Inhibition of CX3CR1

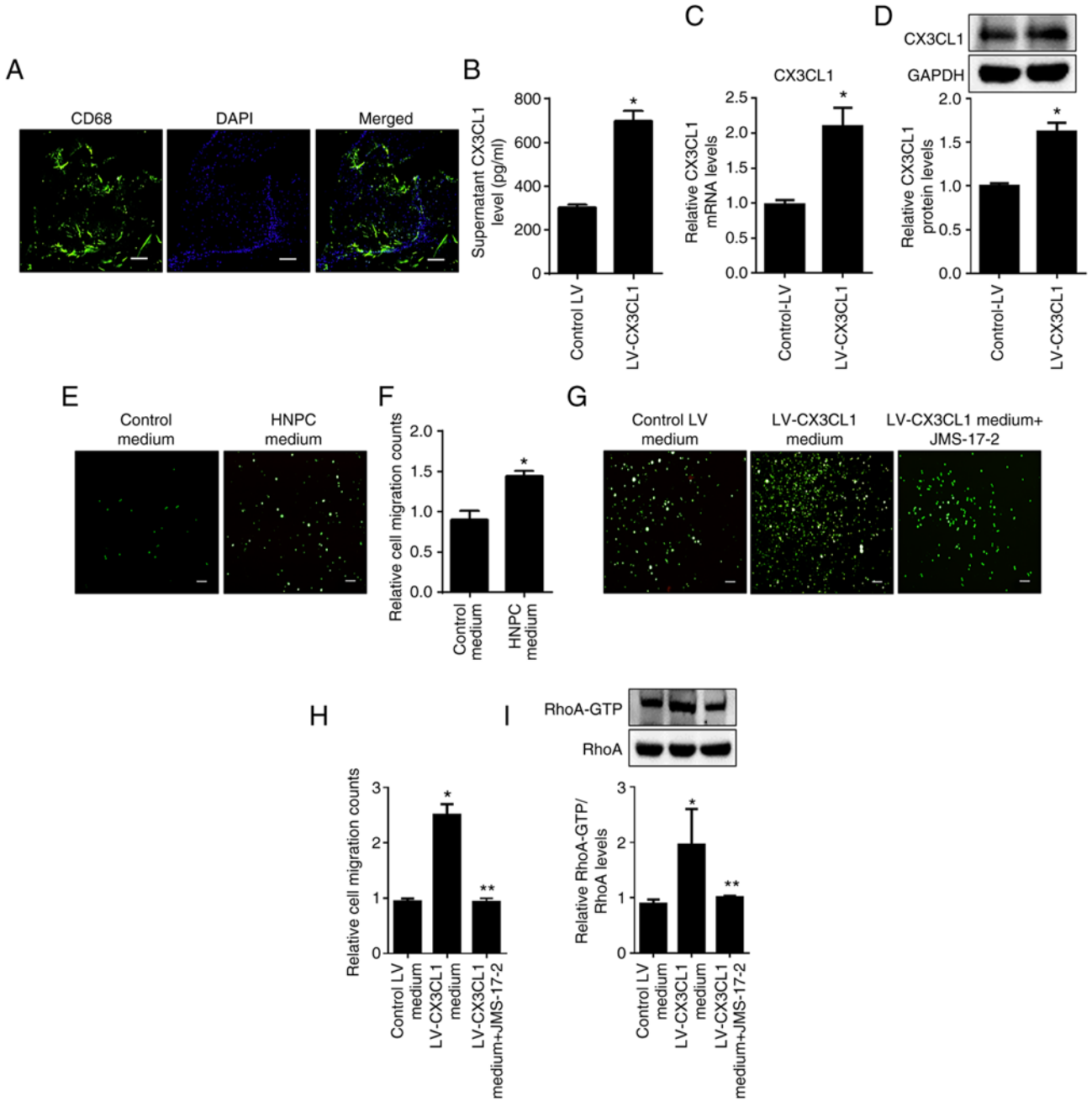

Figure 2. The binding of CX3CL1 to CX3CR1 induces monocyte migration. (A) Detection of the intensity of macrophage marker CD68 in degenerative NPs via immunofluorescence staining. Scale bar, 50 μm. (B) Measurement of medium CX3CL1 level of HNPCs using ELISA. Analysis of (C) mRNA and (D) protein levels of CX3CL1 in HNPCs via reverse transcription-quantitative PCR and western blotting. (E-H) Analysis of immunofluorescence signal of calcein-labelled THP-1-derived monocyte to assess monocyte migration. Scale bar, 50 μm. (I) Analysis of the protein levels of total RhoA and activated RhoA (RhoA-GTP) using western blotting. All data were shown as mean ± SD from three independent experiment with each performed in triplicate. *P<0.05 vs. Control LV or Control LV medium group; **P<0.05 vs. LV-CX3CL1 medium group. CX3CL1, CX3C chemokine ligand 1; CX3CR1, CX3C motif chemokine receptor 1; CD, cluster of differentiation; NPs, nucleus pulposus tissues; LV, lentivirus.

also impaired RhoA signaling in THP-1-derived monocytes (Fig. 2F and G). These data suggested that HNPC-derived CX3CL1 bound to monocyte CX3CR1 followed by the promotion of monocyte migration via RhoA signaling.

CX3CL1/CX3CR1 axis induces M2-like macrophage via JAK2/STAT3 signaling and reduces inflammation of HNPCs. Macrophages act as an important regulator during tissue inflammation via the conversion between pro- and anti-inflammatory phenotypes. The mRNA expression level of M2 marker CD206 significantly decreased (Fig. 3B) whereas M1 marker significantly increased in degenerative NPs (Fig. 3A). The present study next aimed to investigate the role of HNPC-derived CX3CL1 in macrophage polarization and reveal its molecular detail. As shown in Fig. 3C and D, the supernatant from CX3CL1 overexpression HNPCs significantly promoted macrophage polarization into the M2 phenotype while reducing M1-like macrophages, and JMS-17-2 incubation almost eliminated these effects. Moreover, the conditional medium from CX3CL1/CX3CR1 axis-induced M2-like

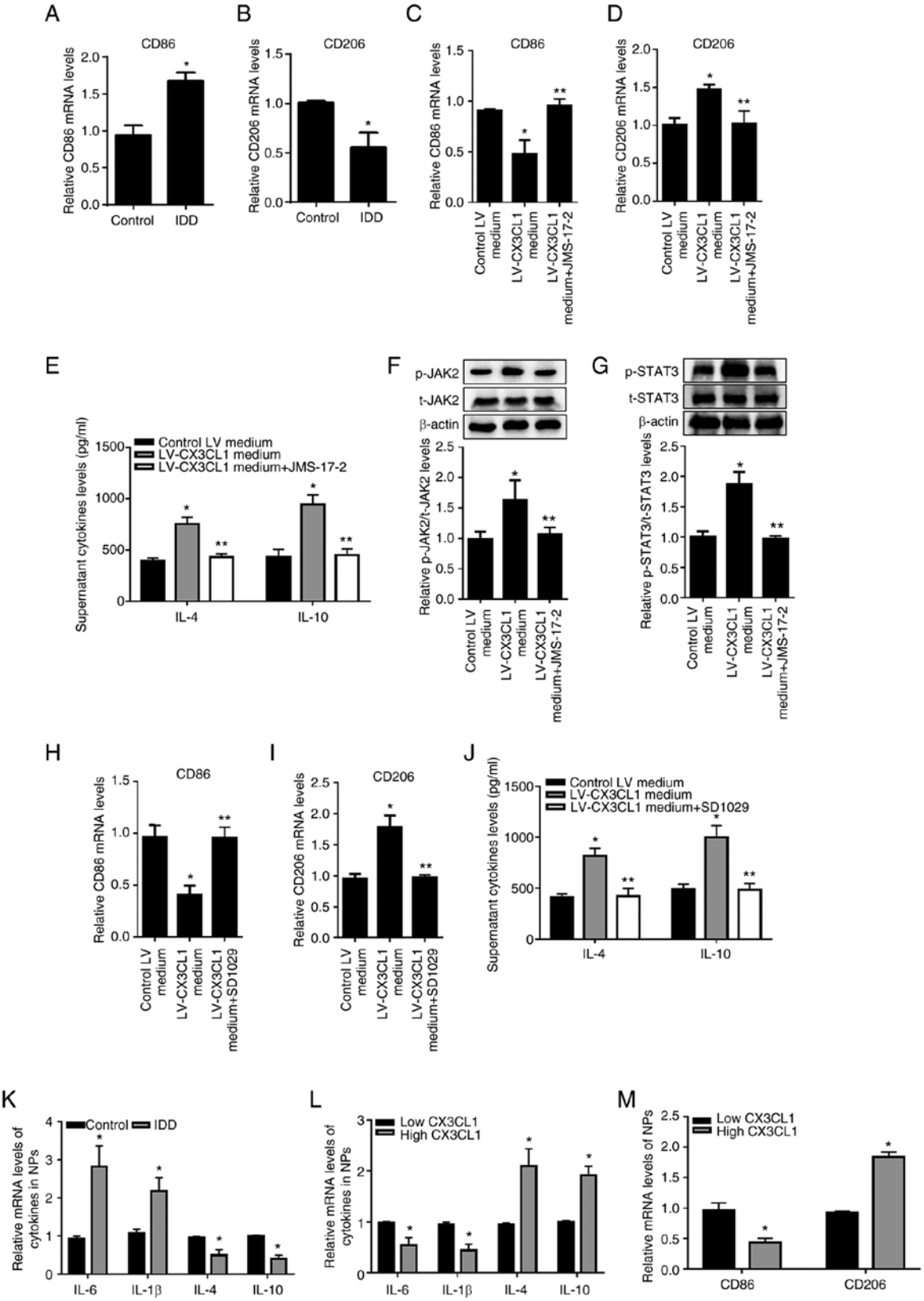

Figure 3. CX3CL1/CX3CR1 axis accelerates M2 macrophage polarization via JAK2/STAT3 signaling and inhibited the inflammatory response in HNPCs. Analysis of (A) M1 (CD86) and (B) M2 (CD206) markers in NPs via RT-qPCR. (C-D) Analysis of M1 (CD86) and M2 (CD206) markers of THP-1-derived macrophages via RT-qPCR. (E) Measurement of media IL-4 and IL-10 level of HNPCs using ELISA. (F and G) Analysis the protein levels of t-JAK2, p-JAK2, t-STAT3 and p-STAT3 via western blotting. Analysis of (H) M1 (CD86) and (I) M2 (CD206) markers via RT-qPCR. (J) Measurement of media IL-4 and IL-10 level of HNPCs using ELISA. (K) Analysis of pro-inflammatory cytokines (IL-1β and IL-6) and anti-inflammatory cytokines (IL-4 and IL-10) markers in NPs via RT-qPCR. Analysis of (L) pro-inflammatory cytokines (IL-1β and IL-6), anti-inflammatory cytokines (IL-4 and IL-10) and (M) M1 (CD86) and M2 (CD206) markers in NPs of low or high CX3CL1 expression via RT-qPCR. All data are mean ± SD from three independent experiment with each performed in triplicate. *P<0.05 vs. Control or Control LV medium or Low CX3L1 groups; **P<0.05 vs. LV-CX3CL1 medium group. CX3CL1, CX3C chemokine ligand 1; CX3CR1, CX3C motif chemokine receptor 1; HNPCs, human nucleus pulposus cells; CD, cluster of differentiation; NPs, nucleus pulposus tissues; RT-qPCR, reverse transcription-quantitative PCR; t-, total; p-, phosphorylated; LV, lentivirus.

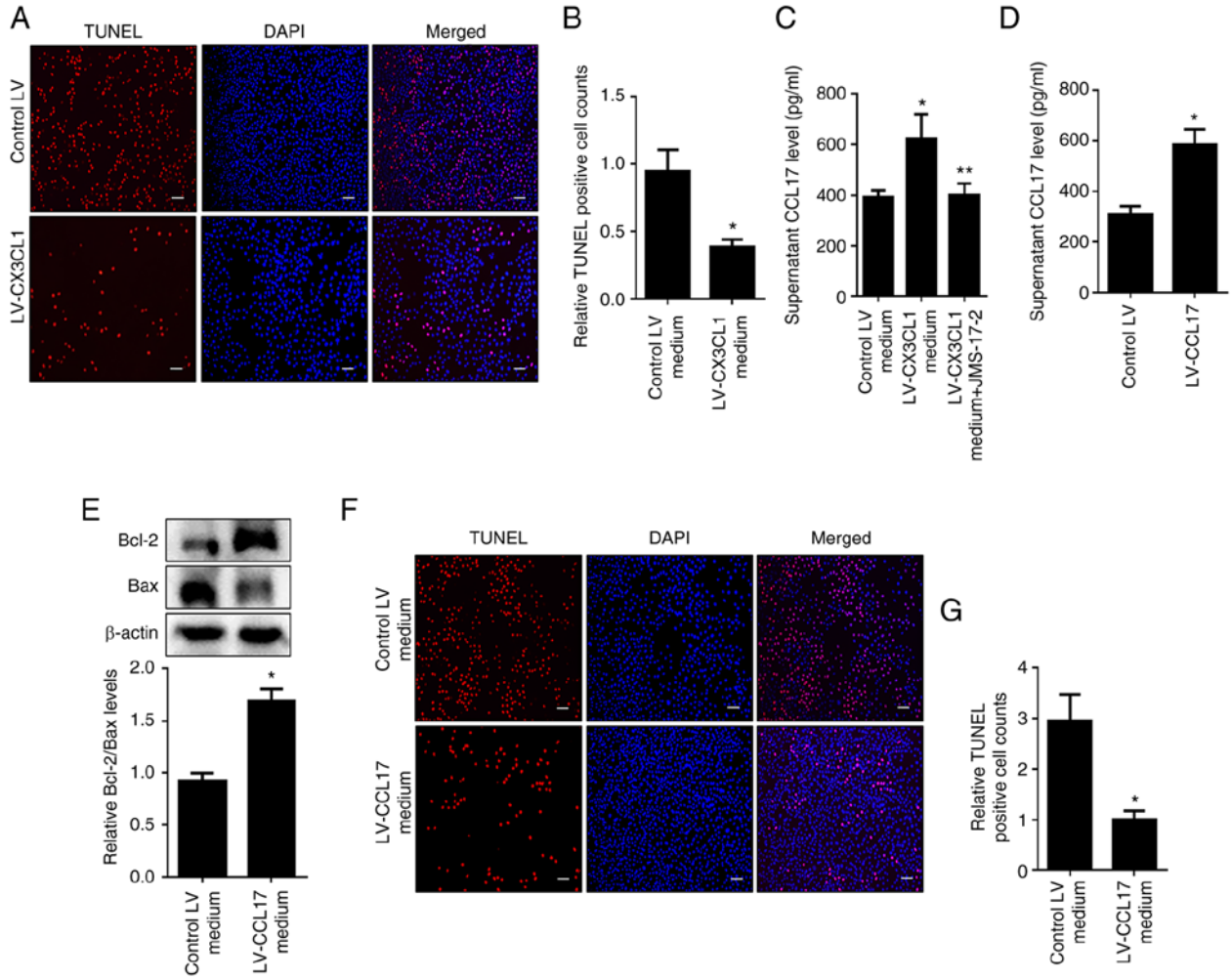

Figure 4. M2 macrophage-derived CCL17 reduced apoptosis of HNPCs. (A and B) Analysis of apoptosis of HNPCs using TUNEL staining, Scale bar, 50 μm. (C) Measurement of CCL17 secretion of THP-1-derived macrophage using ELISA. (D) Measurement of CCL17 overexpression efficiency in THP-1-derived macrophage via ELISA. (E) Analysis of the expression of Bcl-2 and Bax in HNPCs via western blotting. (F and G) Analysis of apoptosis of HNPCs via TUNEL staining. All data are mean ± SD from three independent experiment with each performed in triplicate. *P<0.05 vs. Control LV medium group; **P<0.05 vs. LV-CX3CL1 medium group. HNPCs, human nucleus pulposus cells; CCL17, C-C motif chemokine ligand 17; CX3CL1, CX3C chemokine ligand 1; LV, lentivirus.

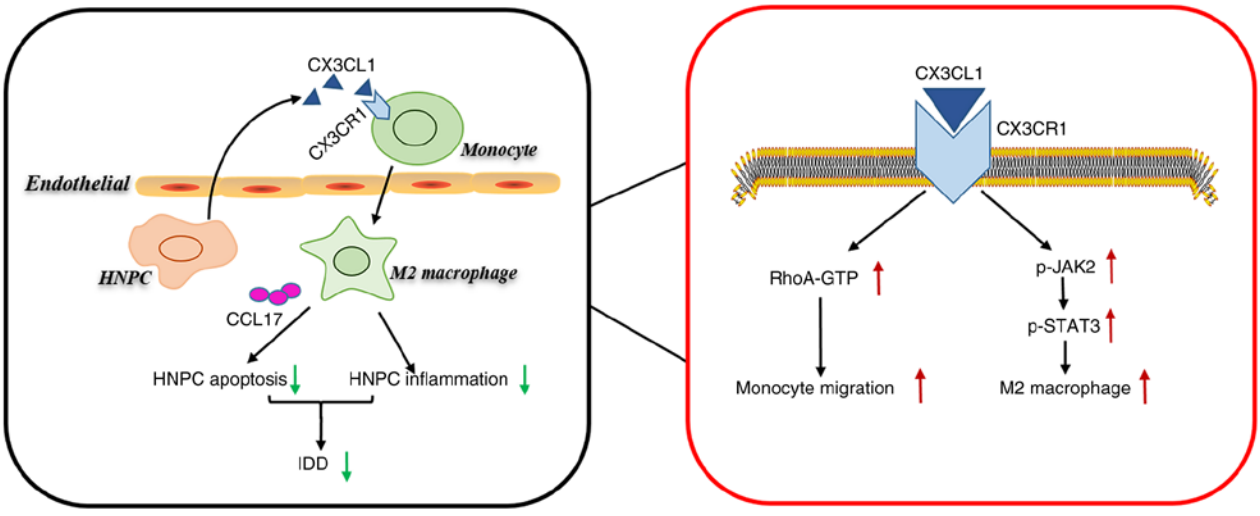

Figure 5. Model for CX3CL1/CX3CR1 axis alleviating IDD progression. HNPC-derived CX3CL1 binds to monocyte CX3CR1 that leads to monocyte migration and M2 macrophage polarization via RhoA and JAK2/STAT3 signaling, respectively. M2-like macrophage promotes the production of anti-inflammatory cytokines from HNPCs and M2 macrophage-secreted CCL17 to inhibit apoptosis of HNPCs. CX3CL1, CX3C chemokine ligand 1; CX3CR1, CX3C motif chemokine receptor 1; IDD, intervertebral disc degeneration; HNPCs, human nucleus pulposus cells; RhoA, Ras homolog family member A; CCL17, C-C motif chemokine ligand 17.

macrophages significantly increased anti-inflammatory cytokines release from HNPCs (Fig. 3E). The activation of classical JAK2/STAT3 signaling is known to occur during M2 polarization (32). The present study suggested that CX3CL1 elevated the phosphorylated levels of JAK2 and STAT3 in THP-1-derived macrophage, while incubation with JMS-17-2 almost reversed these (Fig. 3F-G). Furthermore, JAK2/STAT3 signaling inhibitor SD1029 effectively prevented CX3CL1 overexpression supernatant-induced M2-like macrophages and inhibited M2-like macrophage-promotion of anti-inflammatory cytokines secretion from HNPCs (Fig. 3H-J). In addition, the present study detected increased pro-inflammatory cytokines IL-6 levels and decreased anti-inflammatory cytokines IL-4 and IL-10 levels in NPs of IDD patients (Fig. 3K). Meanwhile, increased pro-inflammatory factors and M1 marker CD86 levels was found in NPs of IDD patients with low CX3CL1 expression group (Fig. 3L and M). These data revealed that the polarization of macrophage in NPs may be dependent on CX3CL1/CX3CR1 axis.

CCL17-mediated the anti-apoptotic effect of M2 macrophage on HNPCs. As macrophages have been reported to be involve in the regulation of cell death (33), the present study aimed to reveal whether an anti-inflammatory type M2-like macrophage serves a role in HNPC apoptosis. As shown in Fig. 4A and B, the data from TUNEL assays indicated that the medium from CX3CL1 overexpression supernatant-incubated macrophages evidently inhibited apoptosis of HNPCs. To further identify the trigger during this process, it was found that JMS-17-2 clearly blocked the increase of CCL17 level in the medium of CX3CL1-overexpressed supernatant-cultured macrophages (Fig. 4C). In addition, the supernatant from CCL17 overexpressed macrophages significantly increased the ratio of Bcl-2 to Bax and reduced apoptosis in HNPCs (Fig. 4D-G). These results indicated that increased CCL17 secretion from M2 macrophages exerted an anti-apoptotic effect on HNPCs.

Discussion

The present study first uncovered a decrease in CX3CL1 expression in the NPs of IDD patients. It provided the first evidence demonstrating that CX3CL1 reduced inflammation and apoptosis in HNPCs (Fig. 5). Mechanistically, the binding of CX3CL1 to monocyte CX3CR1 accelerated monocyte migration via RhoA signaling. In addition, the CX3CL1/CX3CR1 axis activated JAK2/STAT3 signaling to promote M2-like macrophage polarization. The medium from M2 macrophages increased anti-inflammatory cytokine secretion by HNPCs and CX3CL1-induced M2 macrophages reduced HNPC apoptosis by releasing CCL17.

Pro-inflammatory M1 macrophage accumulation promotes the degenerative phenotype of intervertebral discs (18,34,35). Consistent with previous studies, the present study observed macrophage infiltration in degenerative NPs (24). The present study found increased pro-inflammatory cytokine and M1 marker CD86 levels and decreased anti-inflammatory cytokine and M2 marker CD206 levels in degenerative NPs. The important roles of chemokines in different diseases, including IDD (36-38)], by regulating cell chemotaxis are well known. CX3CL1-regulated immune cell recruitment has been revealed, but there is still a lack of evidence about its role and regulatory mechanism in IDD (39,40). The present study detected significantly elevated levels of the M1 macrophage marker CD86 and pro-inflammatory cytokines (IL-1β and IL-6) in IDD patients with low CX3CL1 expression in NPs, indicating that the protective effect of CX3CL1 on intervertebral discs may involve controlling macrophage polarization and alleviating inflammation. The data from the present study suggested that HNPC-derived CX3CL1 induced monocyte migration by increasing cytoskeletal remodeling via CX3CR1/RhoA signaling. Furthermore, the binding of CX3CL1 to macrophage CX3CR1 activated JAK2/STAT3 signaling to induce M2 macrophages. In addition, it was verified that the medium from CX3CL1-induced M2 macrophages increased anti-inflammatory cytokine levels in HNPCs. Although the data provided evidence to support the protective role of CX3CL1 in IDD, it did not verify this *in vivo*. To confirm the clinical value of CX3CL1, the effect of CX3CL1 on IDD of mice will be tested in future work.

In addition to being regulators of the inflammatory response, macrophages also serve a role in apoptosis (26,27). Although abundant macrophages have been examined in degenerative NPs, whether they participate in apoptosis in NPCs was unknown (20,21). Huang *et al* (12) found that CX3CL1 effectively prevented neuronal apoptosis. The present study verified that conditioned medium from CX3CL1-induced M2 macrophages reduced apoptosis in HNPCs. Previous studies verify that M2 macrophages release a large amount of CCL17 and the anti-apoptotic effect of CCL17 has also been confirmed in the nervous system (41,42). The present study found increased secretion of CCL17 by CX3CL1-induced M2 macrophages. In addition, overexpression of CCL17 reduced apoptosis in HNPCs. Revealing the mechanism by which the CX3CL1/CX3CRL1 axis promotes CCL17 secretion is helpful for further understanding the protective effect of CX3CL1 on NPCs.

In short, the present study showed that the CX3CL1/CX3CR1 axis protected against the progression of IDD. Further analysis verified that CX3CL1 bound to CX3CR1 and triggered monocyte migration and M2 macrophage polarization via RhoA and JAK2/STAT3 signaling, respectively. In addition, M2 macrophages not only mitigate inflammation but also prevent apoptosis in HNPCs. Therefore, targeting the CX3CL1/CX3CR1 axis is a new approach for alleviating IDD.

Acknowledgements

Not applicable.

Funding

The present study was supported by the Technology Innovation Guidance Plan of Hunan Province (grant no. 2018SK51709).

Availability of data and materials

The datasets analyzed and/or generated during the present study are available from the corresponding author on reasonable request.

Authors' contributions

XG was responsible for conceptualization, validation, investigation, methodology and manuscript writing. HH was responsible for data curation, software based data analysis, validation, investigation and visualization. MX was responsible for data validation, methodology and project administration. CT gave guidance on experimental technologies and was responsible for data curation and validation. JO was responsible for data curation, validation, investigation, visualization, project administration, manuscript revision and funding support. ZL was responsible for data curation, validation, investigation, visualization, project administration, manuscript revision and funding support. JO and ZL confirm the authenticity of all the raw data. All authors read and approved the final manuscript.

Ethics approval and consent to participate

The present study protocol conformed to the globally accepted regulations on clinical studies involving human data, and approval was conferred by the ethics committee of University of South China (approval no. 2021-ky-41). Written informed consent was obtained from all of the participants or donors' families before using the samples.

Patient consent for publication

Not applicable.

Competing interests

The authors declare that they have no competing interests.

References

1. Peng B, Hao J, Hou S, Wu W, Jiang D, Fu X and Yang Y: Possible pathogenesis of painful intervertebral disc degeneration, Spine 31 560-566, 2006.
2. Adams MA, Freeman BJ, Morrison HP, Nelson IW and Dolan P: Mechanical initiation of intervertebral disc degeneration. Spine (Phila Pa 1976) 25: 1625-1636, 2000.
3. Freemont AJ, Watkins A, Le Maitre C, Jeziorska M and Hoyland JA: Current understanding of cellular and molecular events in intervertebral disc degeneration: Implications for therapy. J Pathol 196: 374-379, 2002.
4. Jia J, Nie L and Liu Y: Butyrate alleviates inflammatory response and NF-κB activation in human degenerated intervertebral disc tissues. Int Immunopharmacol 78: 106004, 2020.
5. Yu H, Liu Y, Xie W, Xie Q, Liu Q and Cheng L: IL-38 alleviates the inflammatory response and the degeneration of nucleus pulposus cells via inhibition of the NF-κB signaling pathway in vitro. Int Immunopharmacol 85: 106592, 2020.
6. Risbud MV, Fertala J, Vresilovic EJ, Albert TJ and Shapiro IM: Nucleus pulposus cells upregulate PI3K/Akt and MEK/ERK signaling pathways under hypoxic conditions and resist apoptosis induced by serum withdrawal. Spine (Phila Pa 1976) 30: 882-889, 2005.
7. Erwin WM, Islam D, Inman RD, Fehlings MG and Tsui FW: Notochordal cells protect nucleus pulposus cells from degradation and apoptosis: Implications for the mechanisms of intervertebral disc degeneration. Arthritis Res Ther 13: R215, 2011.
8. Apostolakis S and Spandidos D: Chemokines and atherosclerosis: focus on the CX3CL1/CX3CR1 pathway. Acta Pharmacol Sin 34: 1251-1256, 2013.
9. Limatola C and Ransohoff RM: Modulating neurotoxicity through CX3CL1/CX3CR1 signaling. Front Cell Neurosci 8: 229, 2014.
10. Wojdasiewicz P, Poniatowski LA, Kotela A, Deszczyński J, Kotela I and Szukiewicz D: The chemokine CX3CL1 (fractalkine) and its receptor CX3CR1: Occurrence and potential role in osteoarthritis. Arch Immunol Ther Exp (Warsz) 62: 395-403, 2014.
11. Aoyama T, Inokuchi S, Brenner DA and Seki E: CX3CL1-CX3CR1 interaction prevents carbon tetrachloride-induced liver inflammation and fibrosis in mice. Hepatology 52: 1390-1400, 2010.
12. Huang ZZ, Li D, Liu CC, Cui Y, Zhu HQ, Zhang WW, Li YY and Xin WJ: CX3CL1-mediated macrophage activation contributed to paclitaxel-induced DRG neuronal apoptosis and painful peripheral neuropathy. Brain Behav Immun 40: 155-165, 2014.
13. Oh IS, Suh DW and Ha KY: Hypertrophy of the ligament flavum in degenerative lumbar stenosis associated with the increased expression of fractalkine (CX3CL1)/CX3CR1 chemokine 54: 380-385, 2013.
14. Yang C, Cao P, Gao Y, Wu M, Lin Y, Tian Y and Yuan W: Differential expression of p38 MAPK α, β, γ, δ isoforms in nucleus pulposus modulates macrophage polarization in intervertebral disc degeneration. Sci Rep 6: 22182, 2016.
15. Liu ZH, Sun Z, Wang HQ, Ge J, Jiang TS, Chen YF, Ma Y, Wang C, Hu S, Samartzis D and Luo ZJ: FasL expression on human nucleus pulposus cells contributes to the immune privilege of intervertebral disc by interacting with immunocytes. Int J Med Sci 10: 1053-1060, 2013.
16. Kim JH, Moon HJ, Lee JH, Kim JH, Kwon TH and Park YK: Rabbit notochordal cells modulate the expression of inflammatory mediators by human annulus fibrosus cells cocultured with activated macrophage-like THP-1 cells. Spine (Phila Pa 1976) 37: 1856-1864, 2012.
17. Park JJ, Moon HJ, Park JH, Kwon TH, Park YK and Kim JH: Induction of proinflammatory cytokine production in intervertebral disc cells by macrophage-like THP-1 cells requires mitogen-activated protein kinase activity. J Neurosurg Spine 24: 167-175, 2016.
18. Ni L, Zheng Y, Gong T, Xiu C, Li K, Saijilafu, Li B, Yang H and Chen J: Proinflammatory macrophages promote degenerative phenotypes in rat nucleus pulpous cells partly through ERK and JNK signaling. J Cell Physiol 234: 5362-5371, 2019.
19. Ling Z, Liu Y, Wang Z, Zhang Z, Chen B, Yang J, Zeng B, Gao Y, Jiang C, Huang Y, *et al*: Single-cell RNA-Seq analysis reveals macrophage involved in the progression of human intervertebral disc degeneration. Front Cell Dev Biol 9: 833420, 2021.
20. Yamagishi A, Nakajima H, Kokubo Y, Yamamoto Y and Matsumine A: Polarization of infiltrating macrophages in the outer annulus fibrosus layer associated with the process of intervertebral disc degeneration and neural ingrowth in the human cervical spine. Spine J 22: 877-886, 2022.
21. Yamamoto Y, Kokubo Y, Nakajima H, Honjoh K, Watanabe S and Matsumine A: Distribution and polarization of hematogenous macrophages associated with the progression of intervertebral disc degeneration. Spine (Phila Pa 1976) 47: E149-E158, 2022.
22. Li C, Xu MM, Wang K, Adler AJ, Vella AT and Zhou B: Macrophage polarization and meta-inflammation. Transl Res 191: 29-44, 2018.
23. Bashir S, Sharma Y, Elahi A and Khan F: Macrophage polarization: The link between inflammation and related diseases. Inflamm Res 65: 1-11, 2016.
24. Nakazawa KR, Walter BA, Laudier DM, Krishnamoorthy D, Mosley GE, Spiller KL and Iatridis JC: Accumulation and localization of macrophage phenotypes with human intervertebral disc degeneration. Spine J 18: 343-356, 2018.
25. Li XC, Luo SJ, Fan W, Zhou TL, Huang CM and Wang MS: M2 macrophage-conditioned medium inhibits intervertebral disc degeneration in a tumor necrosis factor-α-rich environment. J Orthop Res 40: 2488-2501, 2022.
26. Mondragon AA, Betts-Obregon BS, Moritz RJ, Parvathaneni K, Navarro MM, Kim HS, Lee CF, LeBaron RG, Asmis R and Tsin AT: BIGH3 protein and macrophages in retinal endothelial cell apoptosis. Apoptosis 20: 29-37, 2015.
27. Ing DJ, Zang J, Dzau VJ, Webster KA and Bishopric NH: Modulation of cytokine-induced cardiac myocyte apoptosis by nitric oxide, Bak, and Bcl-x. Circ Res 84: 21-33, 1999.
28. Truman LA, Ford CA, Pasikowska M, Pound JD, Wilkinson SJ, Dumitriu IE, Melville L, Melrose LA, Ogden CA, Nibbs R, *et al*: CX3CL1/fractalkine is released from apoptotic lymphocytes to stimulate macrophage chemotaxis. Blood 112: 5026-5036, 2008.
29. Gevrey JC, Isaac BM and Cox D: Syk is required for monocyte/macrophage chemotaxis to CX3CL1 (Fractalkine). J Immunol 175: 3737-3745, 2005.

30. Li XC, Luo SJ, Fan W, Zhou TL, Tan DQ, Tan RX, Xian QZ, Li J, Huang CM and Wang MS: Macrophage polarization regulates intervertebral disc degeneration by modulating cell proliferation, inflammation mediator secretion, and extracellular matrix metabolism. Front Immunol 13: 922173, 2022.
31. Liu B, Jiang Q, Chen R, Gao S, Xia Q, Zhu J, Zhang F, Shao C, Liu X, Li X, *et al*: Tacrolimus ameliorates bleomycin-induced pulmonary fibrosis by inhibiting M2 macrophage polarization via JAK2/STAT3 signaling. Int Immunopharmacol 113: 109424, 2022.
32. Li X, Luo J, Li Y, Jia L, Li Y, Ye S, Liu L, Yu Y, Lu Y and Luan Y: Macrophage-derived exosomes in TLR9$^{-/-}$ mice ameliorate sepsis-induced mitochondrial oxidative stress and apoptosis in cardiomyocytes. Oxid Med Cell Longev 2022: 5719974, 2022.
33. Zhang S, Wang P, Hu B, Liu W, Lv X, Chen S and Shao Z: HSP90 inhibitor 17-AAG attenuates nucleus pulposus inflammation and catabolism induced by M1-polarized macrophages. Front Cell Dev Biol 9: 796974, 2021.
34. Zhao F, Guo Z, Hou F, Fan W, Wu B and Qian Z: Magnoflorine alleviates 'M1' polarized macrophage-induced intervertebral disc degeneration through repressing the HMGB1/Myd88/NF-κB pathway and NLRP3 inflammasome. Front Pharmacol 12: 701087, 2021.
35. Phillips KL, Cullen K, Chiverton N, Michael AL, Cole AA, Breakwell LM, Haddock G, Bunning RA, Cross AK and Le Maitre CL: Potential roles of cytokines and chemokines in human intervertebral disc degeneration: Interleukin-1 is a master regulator of catabolic processes. Osteoarthritis Cartilage 23: 1165-1177, 2015.
36. Stich S, Möller A, Cabraja M, Krüger JP, Hondke S, Endres M, Ringe J and Sittinger M: Chemokine CCL25 induces migration and extracellular matrix production of anulus fibrosus-derived cells. Int J Mol Sci 19: 2207, 2018.
37. Ying JW, Wen TY, Pei SS, Su LH and Ruan DK: Stromal cell-derived factor-1α promotes recruitment and differentiation of nucleus pulposus-derived stem cells. World J Stem Cells 11: 196-211, 2019.
38. Klapproth E, Witt A, Klose P, Wiedemann J, Vavilthota N, Künzel SR, Kämmerer S, Günscht M, Sprott D, Lesche M, *et al*: Targeting cardiomyocyte ADAM10 ectodomain shedding promotes survival early after myocardial infarction. Nat Commun 13: 7648, 2022.
39. Komissarov A, Potashnikova D, Freeman ML, Gontarenko V, Maytesyan D, Lederman MM, Vasilieva E and Margolis L: Driving T cells to human atherosclerotic plaques: CCL3/CCR5 and CX3CL1/CX3CR1 migration axes. Eur J Immunol 51: 1857-1859, 2021.
40. Hsu AT, Lupancu TJ, Lee MC, Fleetwood AJ, Cook AD, Hamilton JA and Achuthan A: Epigenetic and transcriptional regulation of IL4-induced CCL17 production in human monocytes and murine macrophages. J Biol Chem 293: 11415-11423, 2018.
41. Zhang A, Liu Y, Xu H, Zhang Z, Wang X, Yuan L, Lenahan C, Zhang C, Jiang J, Fang C, *et al*: CCL17 exerts neuroprotection through activation of CCR4/mTORC2 axis in microglia after subarachnoid haemorrhage in rats. Stroke Vasc Neurol 8: 4-16, 2022.